Characterization of Vivianite from Catavi, Llallagua Bolivia

K. A. Rodgers[1], H. W. Kobe[1], and C. W. Childs[2]

[1] Department of Geology, University of Auckland, Auckland, New Zealand, [2] Landcare Research, Lower Hutt, New Zealand

With 4 Figures

Summary

Vivianite from Catavi Mine, Llallagua, Bolivia, has a near ideal composition with traces of Mg, Zn and Mn. Total rare-earth elements are <1 $\mu g/g$. Mössbauer spectroscopy shows $Fe^{III}/(Fe^{II} + Fe^{III})$ is approximately 0.04. $a = 10.030$Å, $b = 13.434$Å, $c = 4.714$Å, $\beta = 102.73°$. The middle-infrared powder spectrum shows H_2O-related bands at 3490, 3290, 3130 cm^{-1} (stretch), 1618 cm^{-1} (bend), 825 cm^{-1} (rock), and at 665 cm^{-1} a possible $M-OH_2$ twist. PO_4 bands occur at 1045–940 cm^{-1} (stretch) and 570–450 cm^{-1} (bend). Corresponding laser Raman microprobe bands occur at 1051 (ms), 986 (m), 948 (vs), 867 (mw), 828 (w), 568, 532, 453 (m), 442 (mw). Weak Raman bands at about 342, 303, 270 (w), 235 (ms), 227 (sh, ms), 196 (ms), 187 (sh, m), 162 (mw), and 126 (m) may arise from lattice vibrations. Differential thermal responses include a major endotherm from 115–235°C with a shoulder at 170°C and a maximum at 210°C resulting from loss of structural water combined with oxidation of Fe^{2+}, and two small exotherms with maxima at 605 and 780°C related to structural transformations.

Zusammenfassung

Charakterisierung des Vivianits von Catavi, Llallagua, Bolivien

Vivianit von der Catavi Mine, Llallagua, Bolivien zeigt annähernd ideale Zusammensetzung mit Spuren von Mg, Zn und Mn. Der gesamte Gehalt an seltenen Evol-Elementen ist <1 ppm. Die Mössbauer Spektroskopie liefert ein $Fe^{3+}/(Fe^{2+} + Fe^{3+})$ Verhältnis von ungefähr 0.04. $a = 10.030$, $b = 13.434$, $c = 4.714$ Å, $\beta = 102.73°$. Das Infrarot-Pulverspektrum zeigt dem H_2O zuzuordnende Banden bei 3490, 3290, 3130 cm^{-1} (Streckschwingungen), 1618 cm^{-1} (Deformationsschwingung), 825 cm^{-1} (Schaukelschwingung) und eine mögliche $M-OH_2$ Torsionsschwingung bei 665 cm^{-1}. PO_4 Banden liegen bei 1045–940 cm^{-1} (Streckschwingung) und 570–450 cm^{-1} (Deformations-

schwingung). Entsprechende Banden der Laser Raman Mikrosonde liegen bei 1051 (mst), 986 (m), 948 (sst) 867 (mschw), 828 (schw), 568, 532, 453 (m), 442 (mschw). Raman Banden bei etwa 342, 303, 270 (schw), 235 (mst), 227 (Schulter, mst), 196 (mst), 187 (Schulter, m), 162 (mschw) und 126 (m) können auf Gitterschwingungen zurückgeführt werden. Differential-thermoanalytische Untersuchungen zeigen einen endothermen Bereich von 115–235 °C mit einer Schulter bei 170 und einem Maximum bei 210 °C, was auf den Verlust von strukturellem Wasser, das an eine Oxidation des Fe^{2+} gebunden ist, zurückzuführen ist; zwei auf strukturelle Transformationen zurückzuführende exotherme Maxima liegen bei 605 und 780 °C.

Introduction

Vivianite, $Fe_3(PO_4)_2.8H_2O$, is found in many low-temperature hydrothermal and freshwater sedimentary deposits. Its rapid oxidation and accompanying impressive colour change from colourless to pale green to dark greenish-blue has given it some notoriety. Divers accounts include general characteristics and details of physical and chemical properties of the mineral from various occurrences (e.g. *Bocchi* et al. 1971; *Zwann* and *Kortenbout van der Sluys*, 1971; *Dobra* and *Duda*, 1976; *Figueiredo* et al. 1984; *Henderson* et al. 1984; *Riezebos* and *Rappol*, 1987; *Manning* et al. 1991).

Vivianite and associated phosphates are common in various Andean subvolcanic polymetallic hydrothermal vein deposits e.g. Cerro de Pasco, Peru (*Petersen*, 1965), and from mines in the Oruro and Llallagua districts of Bolivia (*Sugaki* et al. 1981; *Bancroft*, 1984), but are only cursorily described. The donation of a vivianite crystal fragment from Catavi Mine, Llallagua, Bolivia, by Ingo Alberto Sánchez of La Paz, provided the opportunity to obtain details of physical and chemical parameters for a single Andean specimen and to compare these with literature values to obtain an improved idea of its constitution. Properties determined include chemical composition, including Fe^{II}/Fe^{III} from Mössbauer spectroscopy, unit cell size, infrared and Raman spectra, and differential thermal response. The analysed specimen is presently held in the mineralogy collection of the Australian Museum, Sydney, specimen number D49263.

Occurrence

The Catavi Mine lies 80 km southeast of Oruro in the Llallagua district of the tin-silver province of Bolivia. Here mineralised veins occur mainly within a locally brecciated quartz porphyry stock of Tertiary age intruding Silurian greywackes. A pervasive hydrothermal alteration, i.e. tourmalinization, silicification, kaolinization, sericitization, surrounds the vein systems. The principal minerals are cassiterite, quartz, and pyrite. Lesser amounts of marcasite, arsenopyrite, pyrrhotite, wolframite, bismuthinite, stannite, sphalerite, tourmaline, siderite, kaolin, franckeite, apatite, vivianite, paravauxite, and vauxite complete the paragenesis (*Sugaki* et al. 1981). Regionally four stages of telescoped mineral deposition have been recognised from an early high temperature (530–400°C) cassiterite (with apatite) association to a late phase low temperature (<70°C) sulphosalts with vivianite and other hydrous phosphates association. According to *Turneaure* (1971, p.220): "wavellite and vivianite may be hypogene or supergene; the other hydrous phosphates are supergene".

Identification of some opaque minerals intergrown with the studied vivianite help to establish its paragenetic relationship. Small idiomorphic pyrite crystals have grown along the surface of vivianite, while colloform, melnikovite-type pyrite forms irregular crusts with some marcasite, partly infilling shrinkage cracks in a colloform ferriferous-alumina matrix. Sphalerite (with an Fe content of 10–30%) occurs either as solid irregular crystals or as colloform to globular aggregates, partly filling cavities in the pyrite-silica masses. Occasionally thin stannite seams partly overgrow sphalerites. This assemblage indicates a late stage hypogene, low temperature formation of both sulphides and vivianite.

The vivianite crystal consists of a tabular cleavage, 35 × 20 × 12 mm, and originally weighed about 21 g. It exhibits a chatoyancy ranging from BCC 45 Saxe Blue to BCC 191 Cambridge Blue. Very thin, (010), transparent, Cambridge Blue flakes are rimmed by edges of darker Saxe Blue, this colour also pigmenting the edges of (100) and (106) cleavage traces. Slightly thicker, translucent flakes vary throughout from Saxe Blue to BCC 195 Delphinium. Thin flakes along cleavages were selected for detailed instrumental analysis.

Chemical Composition

Spot electron microprobe analyses of a 1 mm^2 polished flake gave average values for FeO of 42.47 and for P_2O_5 of 28.57 wt%, both consistent with the ideal formula (FeO 42.96, P_2O_5 28.31, H_2O 28.73%). All spots proved to have P_2O_5 slightly greater than 28.3%. ΣFeO + MgO + MnO was always less than 42.9%. Traces of magnesium (0.2–0.7%), zinc (0.07–0.38%), and manganese (0.01–0.04%) were detected in nine of the eleven spots probed and may be substituting for Fe^{2+} or, along with arsenic (0.04–1.05%), may be associated with the small grains of sulphides and other minerals noted above, along the edge of the probed flake.

Inductively coupled plasma analysis of 2.1439 g of the vivianite dissolved in 25 ml acid, showed all rare-earth elements to be below the limits of detection, viz., La < 0.6, Ce < 0.6, Nd < 0.7, Sm < 0.7, Eu < 0.05, Gd < 0.16, Dy < 0.12, Yb < 0.07, Lu < 0.02 μg/g. Henderson et al. (1984) failed to detect rare-earth elements in a coarsely crystalline vivianite from N'gaundere and reported very low concentrations in hand-picked crystalline and earthy vivianites from New Zealand Quaternary sediments. This result contrasts with higher values these same authors found in separates of the New Zealand specimens prepared by conventional heavy liquid and magnetic separation techniques, but which are comparable to those reported by Roaldset and Rosenquist (1971) for vivianite from Lake Åsrum, Norway. Henderson et al. (1984) noted that chondrite-normalised rare-earth trends for both their higher set of values and Roaldset and Rosenquist's data, paralleled rare-earth trends derived for the respective host rocks, suggesting that all this group of vivianite analyses could be contaminated by host rock materials. Reliable analyses of uncontaminated vivianites show a total rare-earth content of < 1 μg/g.

Mössbauer Spectroscopy

Mössbauer spectra were obtained on a 512-channel Cryophysics microprocessor-based instrument with a constant acceleration drive system (sawtooth waveform) and a [57]Co-in-Rh γ-ray source. The procedure used was similar to that described

in *Childs* et al. (1990) with samples confined in perspex holders as described by *Goodman* (1980). The velocity scale was calibrated with respect to natural iron at 293°K and, typically, half-widths of 0.28 mms^{-1} were obtained for the two central peaks. The midpoint of the natural iron spectrum was used to define zero velocity. Mössbauer spectra were fitted with peaks having Lorentzian shapes using a modified version of the AMOSS interactive computer program (*Aldridge*, 1984).

Spectra were obtained for sub-samples of Cambridge Blue flakes prepared in four different ways designed to minimise orientation effects, and to assess and minimise the extent of oxidation during preparation. The first sub-sample, A (20 mg), was ground with an agate mortar and pestle in air, mixed with powdered polyethylene to provide bulk, and immediately clamped with adhesive tape in a perspex holder and placed in the instrument. The second and third sub-samples, B and C (also 20 mg each), were treated similarly, except they were ground under acetone and cyclohexane respectively, before mixing with polyethylene. The fourth sub-sample, D, was a selection of very thin slivers (43 mg) which was mounted in a perspex holder and run at an angle of 54.7° to the γ-ray beam, the angle required to overcome crystal orientation effects (*Goodman*, 1980). Sub-samples A, B, and C presented 3.5 mg Fe cm^{-2} to the γ-ray beam, and D 12 mg Fe cm^{-2}.

All of the Mössbauer spectra obtained resemble those reported for samples which have undergone a minimum of oxidation (*Tricker* and *Ash*, 1979; *Dormann* and *Poullen*, 1980; *McCammon* and *Burns*, 1980). They consist essentially of Fe^{II} resonances together with a small amount of Fe^{III} resonance.

In modelling each of the spectral envelopes, two Fe^{II} doublets were initially fitted, with the widths and dips of the two peaks forming each doublet constrained to be equal, but allowed to vary between doublets. Values obtained for the isomer shifts (IS) and quadrupole splittings (QS) of the corresponding doublets were the same within statistical uncertainty for all sub-samples. All chi-squared values (501 degrees of freedom) were unacceptably large: 1023 for D, 7226 for C, 8778 for B, and 9876 for A. The chi-squared values indicate the increasing insufficiency of a Fe^{II}-only model, and hence an increasing degree of oxidation. Subsequent progressive addition of Fe^{III} doublets produced satisfactory convergence, and acceptable (1% level) chi-squared values for A, B, and C were obtained with three Fe^{III} doublets. For D convergence was not achieved with more than two Fe^{III} doublets and the chi-squared value was unacceptable. Finally, because of the possibility of a small amount of residual orientation in all sub-samples, the spectra were fitted allowing the dips of the peaks of each Fe^{II} doublet to be unequal. This approach, with the inclusion of only one Fe^{III} doublet, produced excellent fits for B, C, and D, though the chi-squared for A, at 617, remained marginally higher than the acceptable 1% value (578).

Results of two of the fits are shown in Fig. 1 and Table 1 for:

(a) the "final" fit for D with two Fe^{II} doublets (dips allowed to be unequal, widths for each pair constrained to be equal) and one Fe^{III} doublet (widths and dips constrained to be equal);

(b) the fit for C with two Fe^{II} and three Fe^{III} doublets (widths and dips for each pair constrained to be equal).

The IS and QS values shown in Table 1 for the two Fe^{II} doublets were the same, within uncertainty, in all of the fits for all of the sub-samples. They are in excellent agreement with values reported for other vivianites by *Dormann* and *Poullen* (1980)
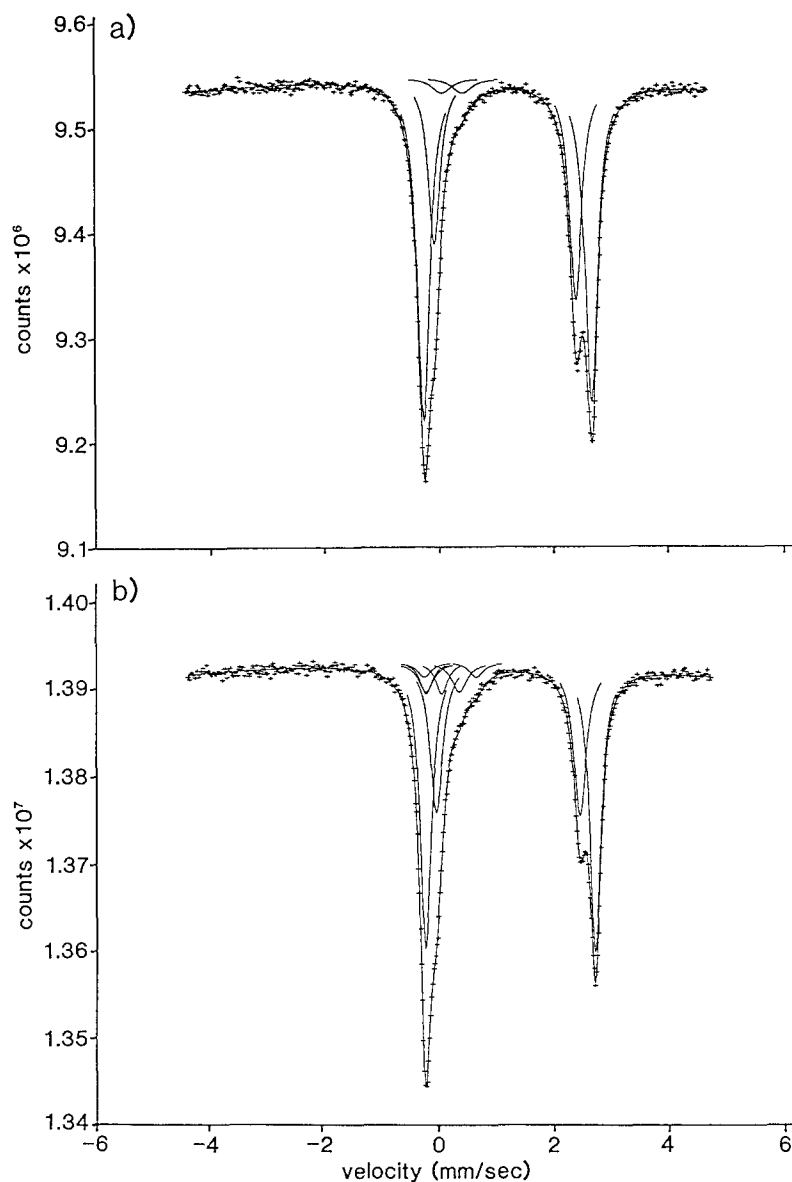
Fig. 1. Mössbauer spectra for Catavi Mine vivianite at 293°K: (a) sub-sample D and (b) sub-sample C; both fitted as described in the text to produce the values shown in Table 1. Points are experimental data; lines show the fitted doublets and spectral envelopes

and *McCammon* and *Burns* (1980). Fe_B^{II}/Fe_A^{II} peak-area ratios, for the "final" fits (corresponding to (a), Table 1) were 1.7(1) for sub-sample A, 1.65(10) for B, 1.85(10) for C, and 1.8(1) for D. These values are slightly lower than that reported by *McCammon* and *Burns* (1980) for an "unoxidized sample". Fe_A^{II} and Fe_B^{II} are attributable to Fe in isolated octahedra and paired octahedra, respectively, within the crystal structure (*Mori* and *Ito*, 1950).

Because of second order effects the number of components observed in Mössbauer spectra is sometimes greater than the number of crystallographic sites. The Fe^{III} resonances reported here, however, make relatively small contributions to the

Table 1. *Mössbauer data for vivianite from Catavi Mine, Bolivia, at $293°K$*[a]

| | (a) Sub-sample D (chi-squared 455) | | | |
	IS	QS	HW	A
Fe_A^{II}	1.18(1)	2.48(1)	0.26(1)	34(1)
Fe_B^{II}	1.22(1)	2.96(1)	0.27(1)	61(1)
Fe^{III}	0.25(4)	0.36(4)	0.43(6)	4(1)
	(b) Sub-sample C (chi-squared 505)			
	IS	QS	HW	A
Fe_A^{II}	1.18(1)	2.50(1)	0.27(1)	31(1)
Fe_B^{II}	1.22(1)	2.95(1)	0.23(1)	52(1)
Fe^{III}	−0.12(11)	0.27(22)	0.25(6)	6(1)
Fe^{III}	0.04(13)	0.58(26)	0.32(7)	7(2)
Fe^{III}	0.17(21)	0.90(43)	0.29(7)	3(1)

[a] Isomer shift (IS), quadropole splitting (QS), and peak width at half height (HW) are given in mm s^{-1}, with IS relative to iron metal at 293°K. Relative doublet areas (A) are given in %. Numbers in parentheses are computed standard deviations on last significant figures. The nature of the sub-samples C and D, the fitting procedure and constraints, and the models used, are described in the text

spectra, and the fits do not allow the number of spectral components nor the values of the parameters to be accurately defined. The peak areas of the "final" fits indicate the following $Fe^{III}/(Fe^{II} + Fe^{III})$ values: 0.04(1) for sub-sample D, 0.08(1) for C, 0.09(1) for B, and 0.13(1) for A. These values indicate the same order of increasing extent of oxidation noted previously. All of the sub-samples which were ground have undergone some oxidation, though those ground under acetone or cyclohexane have undergone less than that ground in air. Although it was possible to fit up to three Fe^{III} doublets in some cases, the uncertainties in the parameters were always very large (e.g. (b), Table 1) and the parameters should not be ascribed to distinct Fe^{III} sites on this evidence alone. When only one Fe^{III} doublet was fitted the peak-width values were usually about twice those obtained for the Fe^{II} peaks. Thus, it appears that there is more than one Fe^{III} site within the structure and/or there is a significant degree of site variability.

Previous studies have focused on the mechanisms of oxidation of vivianite. *Tricker* and *Ash* (1979) confirmed that surface regions of the crystals were less susceptible to oxidation than interior regions, and ascribed this to a preferential dehydration of surface regions producing a lower hydrate which was relatively stable to oxidation. *McCammon* and *Burns* (1980) proposed a model, which involved the preferential oxidation of Fe^{II} in A sites relative to B sites, to account for their finding that grinding in air produced an increase in the peak-area ratio, Fe_B^{II}/Fe_A^{II}, with Fe^{III} content. *Dormann* and *Poullen* (1980) characterised a range of vivianites and meta-vivianites which they described as partly oxidised vivianites. Their data for natural samples do not support an increase in Fe_B^{II}/Fe_A^{II} values with Fe^{III}. In this, and later work (*Dormann* et al. 1982), they included three Fe^{III} sites in their Mössbauer spectral models.

X-ray Powder Diffraction Results

X-ray diffraction analysis was undertaken using a Phillips diffraction goniometer fitted with a graphite monochromator and employing Cu–Kα radiation. Care was taken to select those portions of a small cleavage fragment which were pale Cambridge Blue and therefore presumably had least oxidation. Crushing and grinding was done under n-hexane to minimise any further oxidation, although some darkening of the powder occurred during the subsequent x-ray exposure.

Resulting powder diffraction data are listed in Table 2 along with hkl values calculated by least squares regression analysis using Benoit's (1987) microcomputer version of Appleman and Evans's (1973) programme.

Calculated unit cell constants for 35 reflections are $a = 10.030\text{Å}$, $b = 13.434\text{Å}$, $c = 4.714\text{Å}$, $\beta = 102.73°$. These values are close to those given in U.S. National Bureau of Standards Monograph 25:38 (1979) for artificial $Fe_3(PO_4)_2.8H_2O$ determined in a similar manner ($=JCPDS$ Powder Diffraction Data File 30-662): $a = 10.034\text{Å}$, $b = 13.449\text{Å}$, $c = 4.707\text{Å}$, $\beta = 102.65°$. Both results differ from the refined cell calculated by Fejdi et al. (1980) for a single crystal from Huanuni, 50 km southeast of Oruro, Bolivia, based on 1887 reflections obtained from three dimensional x-ray diffraction procedures. These authors obtained $a = 10.086\text{Å}$, $b = 13.441\text{Å}$, $c = 4.703\text{Å}$, $\beta = 104.27°$.

Infrared and Raman Spectra

Middle-infrared absorption spectra of powders prepared from both the less oxidised Cambridge Blue central portion of the sample and from the darker Saxe Blue margin were measured with a Digilab FTS-60 Fourier transform infrared spectrophotometer at a resolution of 4.0. Each portion was ground under n-hexane to minimise

Table 2. X-ray powder diffraction data for vivianite from Catavi Mine, Bolivia

d(Å)	I/I_0	hkl	d(Å)	I/I_0	hkl	d(Å)	I/I_0	hkl
7.89	10	110	2.706	15	$\bar{1}41$	1.883	7	170
6.73	100	020	2.634	5	330	1.793	<1	$\bar{5}30$
4.89	5	200	2.591	8	$\bar{1}50$	1.785	2	$\bar{4}51$
4.55	2	$\bar{1}01$	2.528	5	141	1.771	5	071
4.35	2	011	2.447	<1	400	1.678	40	080
4.07	12	130	2.418	<1	301	1.660	<1	$\bar{3}52$
3.844	2	101	2.318	8	051	1.597	2	451
3.762	<1	$\bar{1}21$	2.274	1	321	1.581	2	550
3.356	7	040	2.230	5	$\bar{3}41$	1.539	4	181
3.337	5	121	2.193	7	$\bar{2}51$	1.476	7	$\bar{5}61$
3.209	12	031	2.073	5	$\bar{3}50$	1.344	16	010.0
2.987	7	$\bar{3}01$	2.040	1	$\bar{2}60$			
2.957	2	211	2.011	5	$\bar{1}61$			
2.767	5	$\bar{2}40$	1.969	<1	411			
2.730	7	$\bar{3}21$	1.932	5	161			

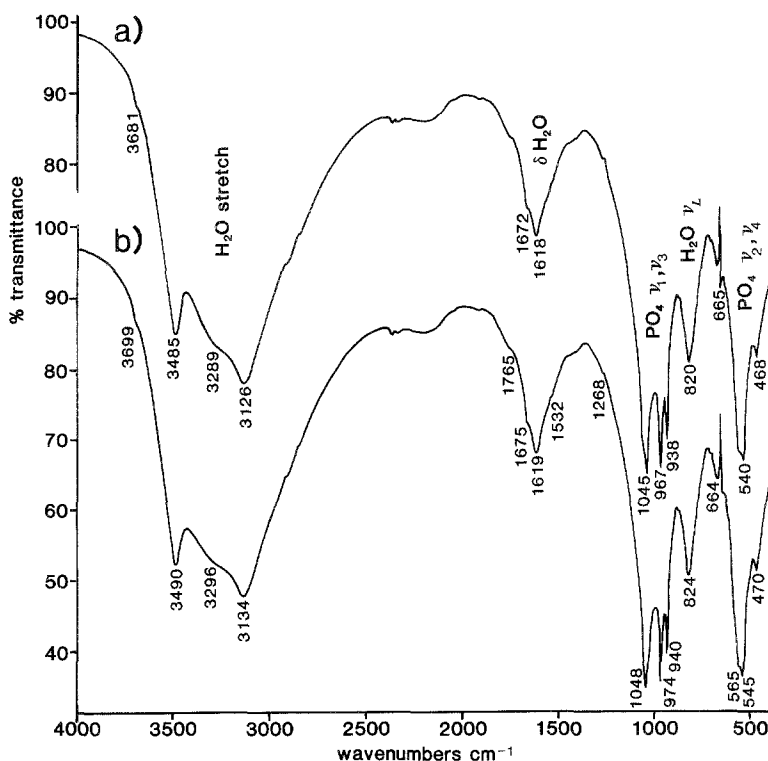$a = 10.030\text{Å}$, $b = 13.434\text{Å}$, $c = 4.714\text{Å}$, $\beta = 102.73°$

Fig. 2. Middle-infrared transmission powder spectra of Catavi vivianite. (a) Cambridge Blue region of crystal cleavage; (b) Saxe Blue margin

oxidation, prepared in a KBr mount, and stored in a vacuum desiccator prior to scanning. Representative results are shown in Fig. 2 and compared with published data in Table 3.

The laser Raman spectra of two different areas of a cleavage flake similar to those used for infrared analysis were recorded by microsampling using a Jobin-Yvon U1000 instrument with 514.5 nm Ar^+ as the exciting line; c. 500 mW laser, 50 mW at ×40 sampling objective of a Nikon microscope. Monochannel Ga–As photomultiplier detectors were employed. Results are given in Table 4 and Fig. 3.

Neither infrared spectrum pattern is substantially different from the other. Both are typical of spectra reported from a range of vivianite specimens which commonly show 6 to 7 major absorptions with weaker bands resolved in some studies (e.g. Chukhrov and Rudnitzkaya, 1966; Brunel and Vierne, 1970; Griffiths, 1970; Farmer, 1974; Gadsden, 1975; Henderson et al. 1984; Piriou and Poullen, 1987). Apart from disparities in relative band intensities near 985, 865 and 450 cm^{-1} that may have arisen from depolarization of the scattered radiation, no substantial differences occur in the Raman spectra recorded for the differently coloured portions of the crystal cleavage. Both resemble spectra obtained by Piriou and Poullen (1984) from an unlocated vivianite crystal oriented such that the A_g modes were amplified. Generally, modes assigned by Piriou and Poullen to B_g are weak or absent in the spectra of the Catavi sample (Table 4.)

As is typical of many hydrated phosphates, the middle-range vibrational spectrum of vivianite contains major bands arising from water and phosphate along

Table 3. *Infrared spectral data for vivianite from Catavi Mine, Bolivia*

Sample 1		Sample 2		Gadsden (1975)		Henderson et al. (1984)	
cm^{-1}	I	cm^{-1}	I	cm^{-1}	I	cm^{-1}	I
3681	88	3699	87				
H_2O stretching							
3485	56	3490	53	3480 − 3400	m, sh	3420 − 3470	vvs
3289	54	3296	55	3200	?	(3300	vs)
3126	49	3133	48	3065	s, b	3100 − 3180	vvs
H_2O in-plane bending							
1672	74	1675	73				
1618	70	1619	68	1635 − 1595	m, b	1630 − 1595	m-w
		1531	76				
PO^4 stretching							
1045	37	1048	35	1040	vs, b	}	vs
967	38	974	37	990 − 970	m, sh	}1050 − 940	vs
938	41	941	4			}	s
librational v_L restricted rotational/rocking vibration of H_2O							
820	52	824	51	890	w, sh	830 − 760	mw
				872	w, sh		
				794	?		
$M-OH_2$ twist							
665	68	664	69				
655	40	654	50				
PO_4 bending and $Fe-OH_2$ wag							
568	40	565	38	590	m, b	}	vs
540	38	545	37	560	b, sh	} 560 − 475	s
500	53	502	58			}	m
468	53	470	52	475	vw	}	w

with those resulting from cation-O interactions (cf. *Levitt* and *Condrate*, 1970; *Braithwaite*, 1988). Vibrations associated with water have been assigned by *Piriou* and *Poullen* (1987) in a polarized infrared reflectivity study of a vivianite single crystal from Anloua: $v_3(W_I) = 3125$ cm^{-1}, $v_1'(W_{II}) = 3260$ cm^{-1}, $v_3'(W_{II}) = 3475$ cm^{-1}, $v_2 = 1620$ cm^{-1}, where W_I and W_{II} are water molecules in the equatorial planes of Fe_I and Fe_{II} octahedral sites respectively. The Catavi H_2O stretching bands show well defined maxima at c. 3490 and 3130 cm^{-1} and a distinct shoulder at c. 3290 cm^{-1}. The spectra closely resemble a powder spectrum of Anloua vivianite given by *Piriou* and *Poullen* (1987, Fig. 11) and that obtained from well crystallised vivianite from N'gaundere, Cameroun, by *Henderson* et al. (1984, Fig. 3). The overall stretching band shape is consistent with the limited amount of oxidation the specimen has

Table 4. *Raman spectral data for vivianite from Catavi Mine, Bolivia and an unlocated specimen from Piriou and Poullen (1984). Assignments from Piriou and Poullen (1984) but see text*

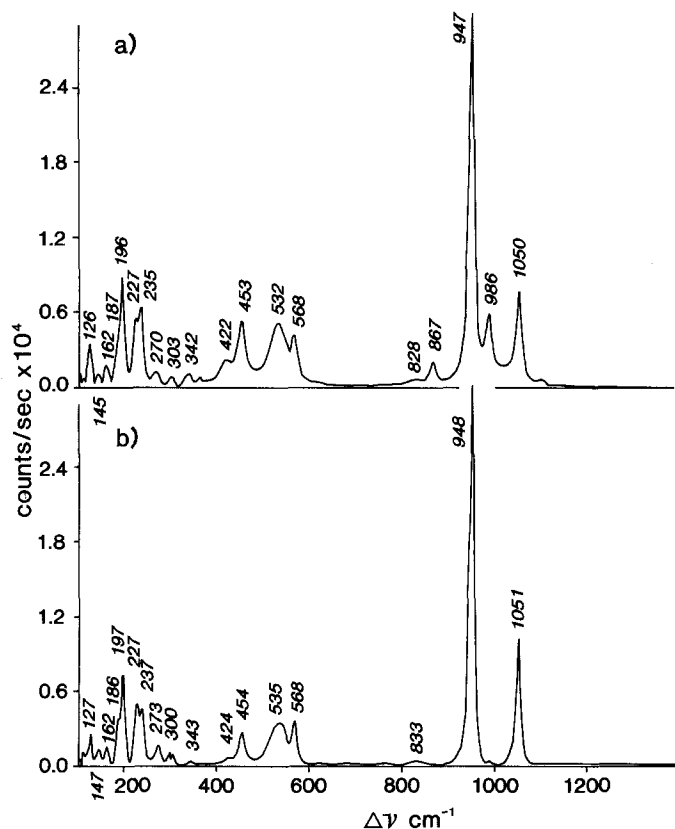| Catavi Mine		Piriou & Poullen	Assignment	
cm^{-1}	I	cm^{-1}	C_{2h}	T_d
1050	3	1052.9	A_g	v_3 PO_4
(1013)	<1	1018	B_g	v_3 PO_4
986	2	990	A_g	v_3 PO_4
947	10	950.5	A_g	v_1 PO_4
867	1	842	A_g	$H_2O{-}Fe$
(828)	<1	833	A_g	$H_2O{-}Fe$
		813	A_g	
		790	B_g	Fe/H_2O
(692)	w	690	B_g	Fe/H_2O
(618)	w	620	A_g	v_4 PO_4?
		593	B_g	Fe/H_2O
		580	B_g	v_4 PO_4
568	2	571.5	A_g	v_4 PO_4
		546.5	B_g	Fe/H_2O
532	2	539	A_g	v_4 PO_4 &/or Fe/H_2O
		525	B_g	Fe/H_2O
453	2	457.5	A_g	v_2 PO_4
422	1	424.5	B_g	v_2 PO_4
365	<1			
342	<1	344		
		307		
303	<1	302		
		274		
270	<1	272		
		242		
235	2	239		
227	2	228		
		222		
		203.6		
		199		
196	3	197		
		172		
162	<1	166		
		153.6		
		149		
145	<1	142		
126	1	130.5		
		79.5		

Fig. 3. Laser Raman microprobe spectra of Catavi vivianite from 100–1300 cm^{-1}. (a) Cambridge Blue centre of crystal cleavage; (b) Saxe Blue margin

undergone (*Henderson* et al. 1984; *Piriou* and *Poullen*, 1987). A small shoulder in both Catavi spectra at c. 3690 cm^{-1} may indicate the presence of a minor amount of non-structural water.

The maximum of the H_2O in-plane bending band (c. 1618 cm^{-1}) for both Catavi spectra, occurs at a frequency typical of vivianite and small shoulders on either side of this band also lie within the range reported for this band (1635–1595 cm^{-1}: *Gadsden*, 1975; *Henderson* et al. 1984).

The medium but well defined infrared band at c. 825 cm^{-1} has been ascribed by *Henderson* et al. (1984) to the librational v_L restricted rotational/rocking vibration of H_2O (cf. *Ross*, 1974, p.402.) *Braithwaite* (1988) tentatively assigned similar bands in the 800–840 cm^{-1} region of hydrated zinc phosphates to ZnO–H out-of-plane bending although parahopeite, which has an absorption band at 805 cm^{-1}, lacks non-water OH. *Piriou* and *Poullen* (1984, p.346) interpreted Raman bands at 833 and 842 cm^{-1}, which were observed only for parallel polarizations, as "probably associated with highly symmetric vibrations of octahedral and double octahedral entities, involving especially motions of water molecules."

A very weak band at 665 cm^{-1} has not previously been reported in the infrared spectrum of vivianite. *Braithwaite* (1988) noted a similar line in the spectra of hydrated zinc phosphates that was absent in the non-hydrated tarbuttite. He assigned it to a coordinated $M-OH_2$ twist.

The T_d site symmetry of the free PO_4^{3-} ion is reduced in vivianite (*Fejdi, Poullen* and *Gasperin*, 1980) and site-group degeneracies are lifted. Assignments of the vibrations of the distorted tetrahedron on the basis of the T_d point group must be made with caution (cf. *Levitt* and *Condrate*, 1970; *Piriou* and *Poullen*, 1984).

Three maxima occur at c. 1045–940 cm^{-1} in the Catavi spectra, consistent with PO_4 stretching. Three infrared active v_3 bands could be expected in this region for C_{2h}. However, a lowering of the molecular symmetry may allow the appearance of the otherwise forbidden v_1, perhaps concealed under, or merged alongside, a v_3 absorption. The intense Raman line at 947 cm^{-1} can be assigned to the v_1 symmetric stretch with the weaker bands at 1050 and 986 cm^{-1} arising from the v_3 antisymmetric stretch. "In spite of the lowering of symmetry due to the site and the field correlation, v_1 is expected to be more intense in A_g than the v_3 components in B_g and A_g, in contrast to the situation in the infrared spectra" (*Piriou* and *Poullen*, 1984, p.344).

Medium weak bands in the infrared between c. 450 to 570 cm^{-1} are assigned to v_4 PO_4 bending. Again three maxima are expected with reduced PO_4^{3-} symmetry and the infrared spectra for the Catavi vivianite both show a multiple band with maxima at c. 565 and 545 cm^{-1} and with a shoulder at c. 500 cm^{-1}. These maxima occur at slightly lower frequencies than reported for other vivianites. The corresponding Raman lines lie at 568 cm^{-1} with one medium broad band at 532 cm^{-1}. Although *Braithwaite* (1988) assigned three strong infrared maxima in this region in the spectrum of spencerite to v_4, he also noted that a coordinated water wag had been recorded at 541 cm^{-1} and at 555 cm^{-1} for hydrated zinc sulphate and the possibility that a similar $Fe-OH_2$ wag exists in vivianite can not be discounted. *Piriou* and *Poullen* (1984) regarded a broad band at 539 cm^{-1} as possibly arising from both v_4 and iron-water interactions.

The symmetrical v_2 bend for PO_4 lies at 420 cm^{-1} in the isolated ion. The range can be extended due to interactions with cations and changes in the crystal structure. *Levitt* and *Condrate* (1970) assigned a very weak infrared band at 436 cm^{-1} to v_2, the strength of which was consistent with its forbidden nature. However, *Braithwaite* (1988) noted that the spectra of spencerite, parahopeite and scholzite appear to show only one absorption maximum each in this region as though their site symmetries were C_{2v} or higher. As these vibrations were appreciably stronger than would be expected from an infrared forbidden vibration, he concluded that some other vibration, possibly a $Zn-OH_2$ stretch could be responsible with the v_2 buried beneath. In the Catavi spectra a clear band exists in the Raman at 453 cm^{-1} but none in the infrared.

Weak bands from 300 and 400 cm^{-1} in the Raman may arise from a librational mode(s) of water. Below 300 cm^{-1} the bands probably arise from lattice vibrations (*Griffiths*, 1970; cf. *Piriou* and *Poullen*, 1984).

Thermochemistry

The differential thermal signature of the Catavi vivianite was obtained with a Shimadzu DT-2B thermal analyzer incorporating 4 $Pt-Pt_{90}Rh_{10}$ thermocouples (0.5 mm o.d.) arranged at 90° and using the experimental procedures and conditions given in *Rodgers* and *Henderson* (1986). 100 mg of the Cambridge blue flakes was ground under acetone with 20 mg of ignited alumina to 100–220 μ, and loose packed
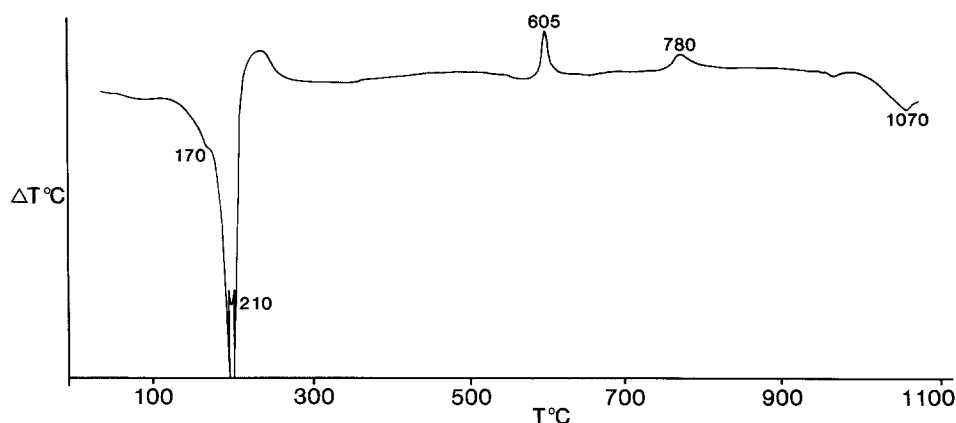
Fig. 4. Differential thermal analytical curve for vivianite from Catavi

in a 6 × 17 mm platinum crucible held in a beryllia holder. Reference material consisted of 100 mg ignited and annealed Al_2O_3. Heating rate was 10°C min^{-1} after 80°C. Furnace atmosphere was air with no turbulence. Two runs were made, one to 1100°C with a sensitivity of ± 100 μV, the second to 600°C with a sensitivity of ± 50 μV.

The differential thermal record (Fig. 4.) shows the typical strong endothermal response of vivianite between 115 and 235°C with a maximum at 210°C. An initial inflection between 40 and 90°C can be ascribed to loss of adsorbed water. *Dormann* et al. (1982) and *Rodgers* and *Henderson* (1986) have interpreted the main response events in this region as arising from continuous, unstaged, dehydration overwritten by a concomitant, continuous, unstaged, exothermal oxidation of Fe^{2+}. Apart from a pronounced shoulder at 170°C, the thermal record of the Catavi vivianite is a smooth curve and it would appear that the differential signal from the endothermic dehydration largely exceeds that from the exothermic oxidation. Similar thermal curves have been described for well crystalline vivianite by *Bocchi* et al. (1971), *Dormann* et al. (1982) and *Rodgers* and *Henderson* (1986) with either a shoulder or small sub-peak in the region 150–200°C.

The Catavi specimen shows a distinct, reproducible exothermic event at 605°C. Vivianite typically shows such a response in the region 657 to 670°C although *Rodgers* and *Henderson* (1986) noted that some specimens show a small additional exotherm between 622 and 628°C. These authors discounted the interpretation of this event as being related to oxidation of Fe^{2+} (e.g. Manly, 1950) and concurred with *Bocchi* et al. (1971) that it represented a further structural transformation.

A second, although smaller and broader exotherm occurs at 780°C in the Catavi specimen. This temperature is typical of vivianites and it is again associated with a phase change (*Rodgers* and *Henderson*, 1986).

Endnote

The data provided give detailed characteristics of one vivianite from an extensive, but not previously described, Andean subvolcanic hydrothermal deposit. A similar, comprehensive data set exists only for unlocated specimens from Anloua that are

not necessarily equivalent (*Bocchi* et al. 1971; *Fejdi* et al. 1980; *Dormann, Gaspérin* and *Poullen*, 1982; *Henderson* et al. 1984; *Dormann* and *Poullen* 1980; *Piriou* and *Poullen*, 1987). Most other published physical data are from vivianite specimens of unknown Fe^{II}/Fe^{III} ratios or lack crystal chemical detail. Before the effect of oxidation on the physical properties of vivianite can be fully appraised, additional data sets are required from specimens from a range of oxidation states, and it need also be noted that routine mineral laboratory measurements of infrared and Raman spectra, thermal characteristics and lattice parameters, seldom have the necessary precision to identify slight differences in oxidation between samples, particularly at low levels of total sample oxidation (cf. *Figueiredo* et al. 1980; *Riezebos* and *Rappol*, 1987, 1989; *Rodgers*, 1989). The Mössbauer results from the present sample indicate it has a very low degree of oxidation representing perhaps the minimal level to be expected from any vivianite sample exposed to air.

Acknowledgements

References

Aldridge LP (1984) AMOSS—a Fortran program for fitting Mössbauer spectra. Chemistry Division DSIR, Lower Hutt, New Zealand, Report CD2336

Appleman DE, Evans HT Jr. (1973) Indexing and least squares refinement of powder diffraction data. U.S. Geological Survey Computer Contribution 20, U.S. National Technical Information Service Document PB2-16188

Bancroft P (1984) Gem and crystal treasures. Mineralogical Record, Tucson, pp 171–175

Benoit P (1987) Adaptation to microcomputer of the Appleman-Evans program for indexing and least squares refinement of powder diffraction data for unit cell dimensions. Am Mineral 72: 1018–1019

Bocchi G, Bondi M, Foresti E, Nannetti MC (1971) Caratteristiche chimiche, termiche, ottiche e roentgenografiche della vivianite di Anloua (Cameroun). Mineralog Petrog Acta 17: 109–133

Braithwaite RSW (1988) Spencerite from Kabwe, Zambia, and the infrared spectroscopy of the Kabwe zinc phosphates. Min Mag 52: 126–9

Brunel R, Vierne R (1970) Infrared spectral studies of minerals. Bull Soc Fr Minér Cristallogr 93: 328–340

Childs CW, Palmer RWP, Ross CW (1990) Thick iron oxide pans in soils of Taranaki, New Zealand. Aust J Soil Res 28: 245–257

Chukhrov FV, Rudnitzkaya ES (1966) On the nature of kerchenite. Proc USSR Acad Sci, Geol Ser 31: 51–56 [In Russian.]

Dobra E, Duda R (1971) Vivianite in the Quaternary sediments of the Vychodoslovenskani-zina Plain. Mineral Slovaca 8: 157–162

Dormann J-I, Gaspérin M, Poullen J-F (1982). Étude structurale de la séquence d'oxydation de la vivianite $Fe_3(PO_4)_2.8H_2O$. Bull Minéral 105: 147–160

Dormann J-I, Poullen J-F (1980) Étude par spectroscopie Mössbauer de vivianites oxydées naturelles. Bull Minéral 103: 633–639

Farmer VC (1974) The infrared spectra of minerals. Mineralogical Society Monograph 4: 539

Fejdi P, Poullen J-F, Gasperin M (1980) Affinement de la structure de la vivianite $Fe_3(PO_4)_2.8H_2O$. Bull Minéral 103: 135–138

Figueiredo MO, Furtado S, Waerenborgh JC (1984) Decomposiçáo térmica da vivianite de Mangualde. Mem Notic Mus Lab Miner Geol Univ Coimbra 98: 83–99

Gadsden JA (1975) Infrared spectra of minerals and related inorganic compounds. Butterworths, London. 277p

Goodman BA (1980) Mössbauer spectroscopy. In: Stucki JW, Banwart WL (eds) Advanced Chemical Methods for Soil and Clay Minerals Research. Reidel, Holland. pp 1–92

Griffiths WP (1970) Raman studies on rock forming minerals Part II: minerals containing MO_3, MO_4 and MO_6 groups. J Chem Soc A: 286–291

Henderson GS, Black PM, Rodgers KA, Rankin PC (1984) New data on New Zealand vivianite and metavivianite. N Z J Geol Geophys 27: 367–378

Levitt SR, Condrate RA Sr (1970) The vibrational spectra of lead apatites. Am Mineral 55: 1562–1575

McCammon CA, Burns RG (1980) The oxidation mechanism of vivianite as studied by Mössbauer spectroscopy. Am Mineral 65: 361–366

Manning PG, Murphy TP, Prepas EE (1991) Intensive formation of vivianite in the bottom sediments of mesotrophic Narrow Lake, Alberta. Can Mineral 29: 77–85

Mori H, Ito T (1950) the structure of vivianite and simplesite. Acta Cryst 3: 1–6

Petersen U (1965) Regional geology and major ore deposits of Central Peru. Econ Geol 60(6): 407–476

Piriou B, Poullen J-F (1984) Raman study of vivianite. J Raman Sp 15(5): 343–346

Piriou B, Poullen J-F (1987) Etude infrarouge des modes vibrationnels de l'eau dans la vivianite. Bull Minéral 110: 697–710

Riezebos PA, Rappol M (1987) Gravel- to sand-sized vivianite components in a Saalian till layer near Borne (The Netherlands). Geol Mijnbouw 66: 21–34

Riezebos PA, Rappol M (1989) Reply. Geol Mijnbouw 68: 257–262

Roaldset E, Rosenquist ITh (1971) Rare earth elements in vivianite from Lake Åsrum. Lithos 4: 417–421

Rodgers KA, Henderson GS (1986) The thermochemistry of some iron phosphate minerals: vivianite, metavivianite, barićite, ludlamite and metavivianite/vivianite admixtures. Thermochim Acta 104: 1–12

Rodgers KA (1989) The thermochemical behaviour of vivianite and vivianite/metavivianite admixtures from Borne (Netherlands) and Mangualde (Portugal). Geol Mijnbouw 68: 257–262

Ross SD (1974) Phosphates and Other Oxy-Anions of Group V. In: Farmer VC (ed) The Infrared Spectra of Minerals. Mineralogical Society Monograph 4: 383–422

Sugaki A, Ueno H, Shimada N, Kitakaze A, Hayashi K, Shima H, Sanjines V, Saavedra A (1981) Geological study on polymetallic hydrothermal deposits in the Oruro District, Bolivia. Sci Rep Tohoku Univ, 3rd series 15(1): 1–52

Tricker MJ, Ash LA (1979) On the anomalous inertness to oxidation of the surface region of vivianite: a [57]Fe conversion electron and transmission Mössbauer study. J Inorg Nucl Chem 41: 891–893

Turneaure FS (1971) The Bolivian tin silver province. Econ Geol 66(2): 215–225

Zwann PC, Kortenbout van der Sluys G (1971) Vivianite crystals from Haren Noord, Brabant Province, the Netherlands. Scr Geol 6: 1–7

Authors' addresses: Associate-Professor *K. A. Rodgers*, Dr *H. W. Kobe*, Department of Geology, University of Auckland, Private Bag 92019, Auckland, New Zealand. Dr. *C. W. Childs*, Landcare Research New Zealand Ltd, Private Bag 31 902, Lower Hutt, New Zealand (formerly DSIR Land Resources, Lower Hutt, New Zealand).